On the Flexibility of the Lewis x, Lewis a, Sialyl Lewis x, and Sialyl Lewis a Oligosaccharides Conformational Analysis in Solution by Molecular Modelling

F. BÍZIK and I. TVAROŠKA*

Institute of Chemistry, Slovak Academy of Sciences, SK-842 38 Bratislava

Received 8 January 1996

The three-dimensional structure and conformational behaviour of the disaccharide α-D-Neu5Ac-(2→3)-β-D-Gal (*I*), two trisaccharides β-D-Gal-(1→3)-[α-L-Fuc-(1→4)]-β-D-GlcNAc (Lewis a, *II*) and β-D-Gal-(1→4)-[α-L-Fuc-(1→3)]-β-D-GlcNAc (Lewis x, *III*), and two tetrasaccharides α-D-Neu5Ac-(2→3)-β-D-Gal-(1→3)-[α-L-Fuc-(1→4)]-β-D-GlcNAc (sialyl Lewis a, *IV*) and α-D-Neu5Ac-(2→3)-β-D-Gal-(1→4)-[α-L-Fuc-(1→3)]-β-D-GlcNAc (sialyl Lewis x, *V*) in solution have been established using molecular modelling methods. The conformations available for each tri- and tetrasaccharide have been based on the minima available for disaccharide constituents of these oligosaccharides. The structure of the minima was calculated by molecular mechanics program RAMM which uses the MM2 force field in conjunction with the Monte Carlo simulation for a determination of the best side group orientations and with the evaluation of solvent effects. Abundances of conformers appear to depend strongly on the solvent. Comparison showed that calculated average vicinal carbon—proton coupling constants $\langle {}^3J_{C,H} \rangle$ are in good agreement with available experimental data. These results imply that the flexibility of these compounds is larger than assumed up to now.

The oligosaccharides related to blood group antigenic determinants and their sialylated derivatives often occur on the cell surface as terminal part of glycoproteins and glycolipids. They are important in many biological events such as antigen—antibody interactions, cell-cell adhesion in inflammatory response and binding of tumour cells in the course of metastasis [1]. The finding [2—4] that tetrasaccharide sialyl Lewis x (α-D-Neu5Ac-(2→3)-β-D-Gal-(1→4)-[α-L-Fuc-(1→3)]-β-D-GlcNAc) is a ligand for ELAM-1 (Endothelial Leukocyte Adhesion Molecule 1) has led to a considerable interest [5—22] in the three-dimensional structure of the sialyl Lewis x and sialyl Lewis a (α-D-Neu5Ac-(2→3)-β-D-Gal-(1→3)-[α-L-Fuc-(1→4)]-β-D-GlcNAc) as well as of their trisaccharide precursors Lewis x (β-D-Gal-(1→4)-[α-L-Fuc-(1→3)]-β-D-GlcNAc) and Lewis a (β-D-Gal-(1→3)-[α-L-Fuc-(1→4)]-β-D-GlcNAc). Most structural data have been obtained from high-resolution NMR spectroscopy (NOE, coupling constants), supplemented by calculations using different molecular modelling methods.

Based on the conformational study using NMR experiments and molecular mechanics calculations in vacuum, it was suggested that only one stable conformer of the sialyl Lewis x exists in aqueous solution [5, 7, 9, 12]. These conclusions are controversial with some experimental and molecular modelling data [15, 16, 22] which indicate a pronounced flexibility for the α-D-Neu5Ac-(2→3)-β-D-Gal linkage. The Lewis x and Lewis a trisaccharide parts are assumed to be rigid. On the other hand, it was recently suggested [23] that the β-(1→4) linkage between Gal and GlcNAc in *N*-acetyllactosamine (β-D-Gal-(1→4)-β-D-GlcNAc) segment may also occur for some time in other conformations than the minimum energy conformation. The evaluation of an influence of solvent on conformational behaviour of carbohydrates still represents a problem in molecular modelling of these molecules. It is noteworthy that most of molecular modelling studies of sialyl Lewis x and sialyl Lewis a and related structures did not take into account solvent effects and the agreement between experiment and calculation was often achieved only after applying constraints. In our previous study [24] we have investigated conformational space available to constituent disaccharides of Lewis x and Lewis a in solution. These results together with the data for the α-D-Neu5Ac-(2→3)-β-D-Gal (*I*) disaccharide provide essential information for conformational analysis of more complex oligosaccharides presented here.

In this paper we report on a detailed conformational analysis of the disaccharide α-D-Neu5Ac-(2→3)-β-D-Gal (*I*), two trisaccharides β-D-Gal-(1→3)-

*The author to whom the correspondence should be addressed.

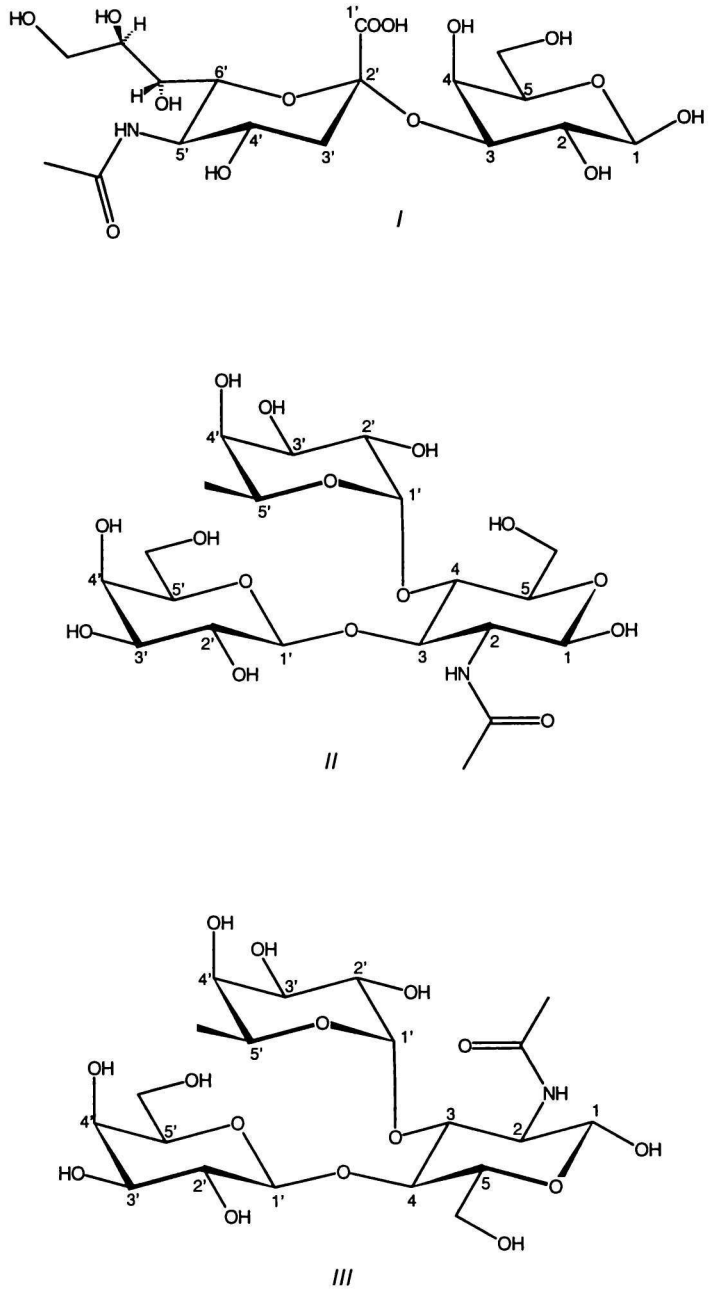

Scheme 1

[α-L-Fuc-(1→4)]-β-D-GlcNAc (Lewis a, *II*) and β-D-Gal-(1→4)-[α-L-Fuc-(1→3)]-β-D-GlcNAc (Lewis x, *III*), and two tetrasaccharides α-D-Neu5Ac-(2→3)-β-D-Gal-(1→3)-[α-L-Fuc-(1→4)]-β-D-GlcNAc (sialyl Lewis a, *IV*) and α-D-Neu5Ac-(2→3)-β-D-Gal-(1→4)-[α-L-Fuc-(1→3)]-β-D-GlcNAc (sialyl Lewis x, *V*) in various environment using molecular modelling methods. Representations of the five oligosaccharide compounds along with the labelling of the atoms are shown in Scheme 1. Four solvents, namely 1,4-dioxane, methanol, dimethyl sulfoxide, and water have been used to characterize the conformational behaviour of these molecules in solution and to estimate differences between vacuum and solution conformational behaviour.

METHODS

Nomenclature

The torsion angles describing rotation around the glycosidic linkages are defined as $\Phi = \Phi$(O-5′—C-1′—O-x—C-x) and $\Psi = \Psi$(C-1′—O-x—C-x—C-(x −1)) or $\Phi^{H} = \Phi^{H}$(H-1′—C-1′—O-x—C-x) and $\Psi^{H} = \Psi^{H}$(C-

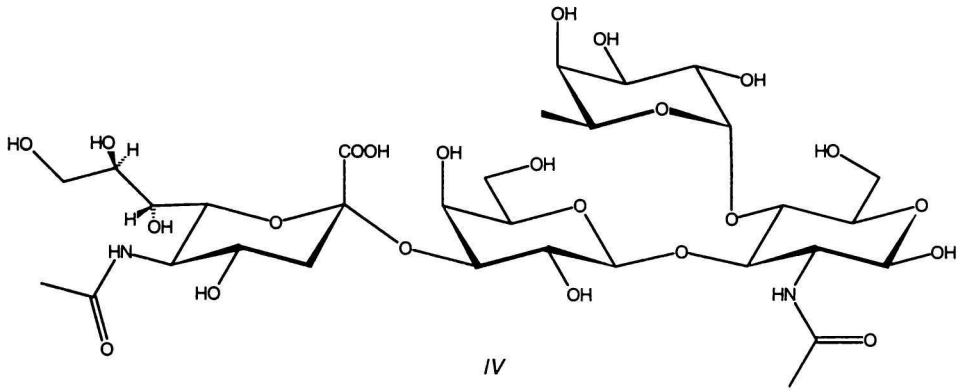

IV

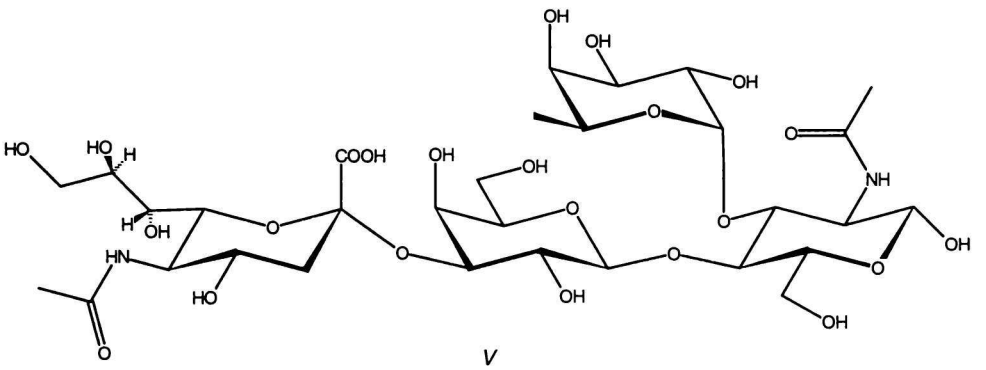

V

Scheme 1 (cont.)

1′—O-x—C-x—H-x), where $x = 3, 4$. The relative orientation of the α-(2→3) linkage in the α-D-Neu5Ac-(2→3)-β-D-Gal fragment is described by torsion angles $\Phi = \Phi$(O-6′—C-2′—O-3—C-3) and $\Psi = \Psi$(C-2′—O-3—C-3—C-2) or $\Phi^{C} = \Phi^{C}$(C-1′—C-2′—O-3—C-3) and $\Psi^{H} = \Psi^{H}$(C-1′—O-3—C-3—H-3).

Computational Methods

The calculations reported here were performed with the RAMM program (RAndom Molecular Mechanics) [25]. The RAMM program employs molecular mechanics method with potential functions and parametrization of the MM2(89) method [26] for calculations of an energy of conformers. The orientation of rotatable groups is treated with the Monte Carlo (MC) based procedure, which is a part of RAMM. For solvent effect calculations, the program uses continuum approach. Here the solvation energy is represented by the sum of cavity, dispersion and electrostatic energy contributions [27]. More detailed description of the program was given in our previous papers [25, 27].

The vicinal heteronuclear and the one-bond carbon—proton coupling constants were calculated by using published Karplus-type equations [28—30]. Statistical mechanics was used to calculate the abundance of conformers and the average values of glycosidic torsion angles and carbon—proton coupling constants [24].

RESULTS

Potential Energy Surface of the α-D-Neu5Ac-(2→3)-β-D-Gal Disaccharide (*I*)

The disaccharide α-D-Neu5Ac-(2→3)-β-D-Gal represents the linkage between the sialic acid and β-D-galactopyranose in many sialylated oligosaccharides. This type of the glycosidic linkage has not been included in our previous investigation [24]. Therefore, at first, a conformational study of this molecule was carried out. The conformational space for the α-D-Neu5Ac-(2→3)-β-D-Gal disaccharide was investigated by a systematic grid search method. The calculation of the (Φ, Ψ) map was performed over the whole range

of torsion angles Φ and Ψ in steps of 20°. For each point on the (Φ,Ψ) map, the orientation of all rotatable groups was refined applying the MC technique within the RAMM. We have found that 2500 MC steps were sufficient to find the lowest-energy orientation for rotatable groups in *I*. Then, the energy of conformers was minimized with constraints on the torsion angles Φ and Ψ in order to obtain the so-called adiabatic (Φ,Ψ) map. Final geometry optimization was performed on local minima found on the (Φ,Ψ) map without constraints on the torsion angles Φ and Ψ.

The adiabatic conformational energy contour map for the disaccharide α-D-Neu5Ac-(2→3)-β-D-Gal is shown in Fig. 1. The contours are drawn at ΔE/(kJ mol^{-1}) 5, 10, 15, 20, 30, 40, 50, and 60 above the global minimum. The overall shape of the map is similar to those reported with different force fields [12, 18, 31, 32]. However, such details as the location and relative energy of minima differ from those previously reported. This is understandable due to differences in the used force fields and calculation procedure. The (Φ,Ψ) map shows that there are several distinct low-energy regions that are accessible for the disaccharide *I*. This suggests an enhanced flexibility about this glycosidic linkage in comparison with other blood group disaccharides [24]. On the other hand, there is a high-energy region at $\Phi^C \approx 0°$, $\Psi^H \approx -120°$ and $\Phi^C \approx 0°$, $\Psi^H \approx 120°$ that is a consequence of the carboxyl group attached to C-2′. Five distinguished low-energy conformations were found on the conformational map within the relative energy 60 kJ mol^{-1}. The minima are separated by energy barriers less than 30 kJ mol^{-1}. The RAMM minimized conformations calculated without constraints gave Φ, Ψ angles of 80.0°, −64.4° for S1, 38.8°, −105.2° for S2, 54.8°, 22.6° for S3, −42.3°, −142.5° for S4, and −163.9°, −68.0° for S5. Description of the observed minima and their energetics are given in Table 1. It can be seen that during the unconstrained minimization the minima remained in their respective low-energy regions. The lowest-energy conformer S1 is characterized by the value $^1J_{C\text{-}3,H\text{-}3}$ = 144.2 Hz. Remaining conformers have similar one-bond coupling constant except S3, where a higher value $^1J_{C\text{-}3,H\text{-}3}$ = 147.4 Hz was obtained. Rather great difference was found between the three-bond carbon—proton coupling constants calculated for two lowest-energy minima S1 ($^3J_{C\text{-}2',H\text{-}3}$ = 1.6 Hz) and S2 ($^3J_{C\text{-}2',H\text{-}3}$ = 5.0 Hz). A small value was also obtained for the conformer S5 ($^3J_{C\text{-}2',H\text{-}3}$ = 1.8 Hz). Based on the energy of conformers, the conformational equilibrium y(S1):y(S2):y(S3):y(S4):y(S5) = 50.3:44.5:4.5:0.6:0.1 can be calculated for this disaccharide.

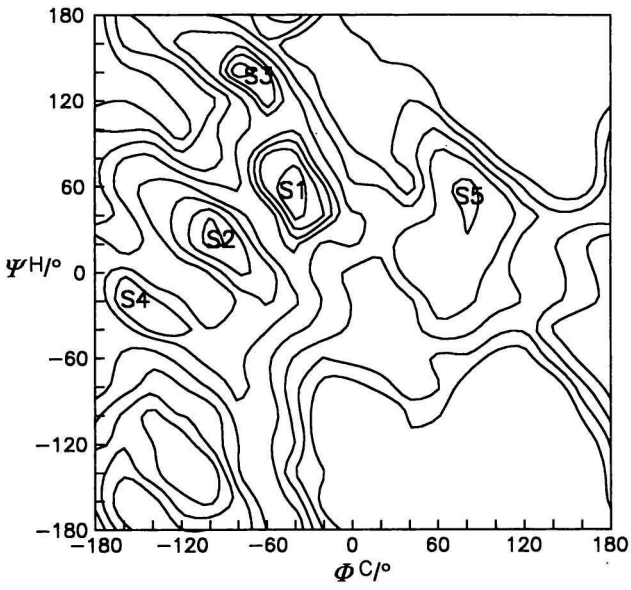

Fig. 1. Relaxed conformational energy map for α-D-Neu5Ac-(2→3)-β-D-Gal (*I*) in vacuum calculated using the RAMM program with the MM2(89) force field. Contours are drawn at ΔE/(kJ mol^{-1}) 5, 10, 15, 20, 30, 40, 50, and 60 above the lowest-energy minimum of the map. Abbreviations designate minima referred to in the text and Table 1.

It is interesting to compare these conformations with those found by other authors for α-D-Neu5Ac-(2→3)-β-D-Gal disaccharide segment [12, 15, 16, 18, 21, 22, 31—38]. The minimum S4 is practically the same as observed in almost all studies for this linkage. Very often this minimum is the only one found. The

Table 1. Numerical Values of Relative Energies ΔE/(kJ mol^{-1}), Dipole Moments μ/D, Torsion Angles Φ^C/°, Ψ^H/°, Φ/°, Ψ/°, and Carbon—Proton Coupling Constants $^1J_{C,H}$/Hz and $^3J_{C,H}$/Hz Calculated for the Local Minima of α-D-Neu5Ac-(2→3)-β-D-Gal (*I*)

	S1	S2	S3	S4	S5
$\{\Delta E\}$	0.00	0.31	6.04	11.14	15.50
$\{\mu\}$	2.6	6.5	3.2	7.1	7.2
$\{\Phi^C\}$	−43.6	−83.8	−70.8	−160.0	80.8
$\{\Psi^H\}$	60.3	19.2	138.6	−22.8	57.4
$\{\Phi\}$	80.0	38.8	54.8	−42.3	−163.9
$\{\Psi\}$	−64.4	−105.2	22.6	−142.5	−68.0
$\{^1J_{C\text{-}3,H\text{-}3}\}$	144.2	144.5	147.4	144.4	144.2
$\{^3J_{C\text{-}2',H\text{-}3}\}$	1.6	5.0	4.1	4.8	1.8

Table 2. Initial and Optimized Glycosidic Torsion Angles $\Phi^H/°$, $\Psi^H/°$, and Relative Energies $\Delta E/(\text{kJ mol}^{-1})$ for Disaccharide Components of Lewis a (*II*) Conformers

		Initial				Optimized				
		β-D-Gal-(1→3)-β-D-GlcNAc		α-L-Fuc-(1→4)-β-D-GlcNAc		β-D-Gal-(1→3)-β-D-GlcNAc		α-L-Fuc-(1→4)-β-D-GlcNAc		
		$\{\Phi^H\}$	$\{\Psi^H\}$	$\{\Phi^H\}$	$\{\Psi^H\}$	$\{\Phi^H\}$	$\{\Psi^H\}$	$\{\Phi^H\}$	$\{\Psi^H\}$	$\{\Delta E\}$
1	A1, K1	31.3	4.2	25.1	−49.1	37.0	21.6	41.0	18.6	0.5
2	A1, K2	31.3	4.2	7.5	179.3	converged to 6				
3	A1, K3	31.3	4.2	−66.7	−61.3	29.0	25.1	−16.5	−40.2	3.0
4	A1, K4	31.3	4.2	171.8	1.2	38.2	13.9	167.0	9.5	47.1
5	A2, K1	179.2	3.7	25.1	−49.1	82.3	56.2	19.1	−45.0	32.1
6	A2, K2	179.2	3.7	7.5	179.3	32.5	25.6	27.2	−169.4	31.6
7	A2, K3	179.2	3.7	−66.7	−61.3	converged to 5				
8	A2, K4	179.2	3.7	171.8	1.2	177.4	−1.1	178.2	8.8	76.3
9	A3, K1	18.6	177.4	25.1	−49.1	34.7	169.9	34.3	−21.7	0.0
10	A3, K2	18.6	177.4	7.5	179.3	44.7	176.2	16.6	176.5	8.5
11	A3, K3	18.6	177.4	−66.7	−61.3	converged to 9				
12	A3, K4	18.6	177.4	171.8	1.2	47.5	168.6	154.0	19.0	57.6
13	A4, K1	75.9	67.6	25.1	−49.1	converged to 5				
14	A4, K2	75.9	67.6	7.5	179.3	converged to 6				
15	A4, K3	75.9	67.6	−66.7	−61.3	75.1	58.2	−59.7	−68.4	50.5
16	A4, K4	75.9	67.6	171.8	1.2	converged to 4				

minima similar to S2, S3, and S5, were also reported for this linkage [32]. The lowest-energy minimum S1 was found [32] only for the disaccharide but the calculated energy was by 8 kJ mol^{-1} higher than that for the lowest-energy conformer. It is noteworthy that in this minimum, the aglycon carbon (C-3) is in *gauche* orientation with respect to the ring oxygen (O-5′). This orientation around the Φ torsion angle corresponds to the one preferred by the exo-anomeric effect [39]. The calculated preference of the S1 minimum is at variance with experimental data [18, 22] from the complex oligosaccharides which were interpreted by the equilibrium between the S2 and S4 conformers. This might suggest that a presence of other substituents in complex oligosaccharides introduces additional interactions between nonlinked residues that may influence the energy of minima found in the disaccharide *I*.

Solution Structure of the Lewis a Trisaccharide (*II*)

In order to explore the conformations of the Lewis a (β-D-Gal-(1→3)-[α-L-Fuc-(1→4)]-β-D-GlcNAc), a systematic search of conformational space was performed. Each glycosidic linkage was put into an initial conformation that corresponded to one of the minima found from the (Φ, Ψ) maps of each disaccharide component [25]. All minima of each disaccharide component were used. Thus, four conformations were used for the β-D-Gal-(1→3)-β-D-GlcNAc (A1—A4) and for the α-L-Fuc-(1→4)-β-D-GlcNAc (K1—K4) linkages, thereby giving a total of 16 combinations of Lewis a conformations. In order to allow all hydroxyl groups, hydroxymethyl side chains, and the acetyl side chain to relax, the MC technique within the RAMM program was applied to each starting conformation. Then a geometry of conformers was optimized without constraints.

A summary of this energy minimization procedure is given in Table 2. Conformations of oligosaccharides are determined in part by the torsional preferences of their constituent glycosidic linkages between monosaccharides. It is expected that glycosidic linkages in more complex oligosaccharides experience similar behaviour as in parent disaccharides. However, in many cases due to repulsive nonbonded contacts between nonlinked monosaccharides in an oligosaccharide, starting conformations do not represent a minimum conformation. For Lewis a, from 16 starting conformers we have obtained 10 minima as a result of energy minimization. Remaining six conformers converged to one of these ten conformers.

Four lowest-energy conformers that were within 30 kJ mol^{-1} are characterized more in detail in Table 3. Six conformers have high relative energies (32—76 kJ mol^{-1}) to be present in equilibrium mixture and therefore were not included in Table 3. Difference in relative energies between two lowest-energy conformers LA1 and LA2 is only 0.51 kJ mol^{-1}. Comparison of the glycosidic torsion angles shows that the difference between these two conformers is mainly in Ψ^H angles. For β-D-Gal-(1→3)-β-D-GlcNAc linkage, a *trans* orientation is present in the LA1 minimum, whereas in the LA2 minimum this linkage is in the *gauche* orientation. The minima LA2 and LA3 differ by orientation around the α-L-Fuc-(1→4)-β-D-GlcNAc linkage. The minimum LA4 with the relative energy 8.48 kJ mol^{-1} has both Ψ^H angles in the *trans* orientation.

Table 3. Numerical Values of Relative Energies ΔE/(kJ mol^{-1}), Dipole Moments μ/D, Torsion Angles $\Phi^H/°$, $\Psi^H/°$, $\Phi/°$, $\Psi/°$, and Carbon—Proton Coupling Constants $^1J_{C,H}$/Hz and $^3J_{C,H}$/Hz Calculated for the Minima of Lewis a (*II*)

	LA1	LA2	LA3	LA4
$\{\Delta E\}$	0.00	0.51	3.03	8.48
$\{\mu\}$	4.2	5.7	4.2	5.4
		β-D-Gal-(1→3)-β-D-GlcNAc		
$\{\Phi^H\}$	34.7	37.0	29.0	44.7
$\{\Psi^H\}$	169.9	21.6	25.1	176.2
$\{\Phi\}$	−84.0	−82.5	−88.9	−74.4
$\{\Psi\}$	56.7	−99.1	−95.3	63.1
$\{^1J_{C\text{-}1',H\text{-}1'}\}$	159.6	159.6	159.5	159.6
$\{^1J_{C\text{-}3,H\text{-}3}\}$	145.8	144.1	144.1	146.1
$\{^3J_{C\text{-}3,H\text{-}1'}\}$	3.9	3.7	4.3	3.0
$\{^3J_{C\text{-}1',H\text{-}3}\}$	6.6	4.9	4.6	6.8
		α-L-Fuc-(1→4)-β-D-GlcNAc		
$\{\Phi^H\}$	34.3	41.0	−16.5	16.6
$\{\Psi^H\}$	−21.7	18.6	−40.2	176.5
$\{\Phi\}$	−85.0	−75.7	−132.8	−100.1
$\{\Psi\}$	100.8	137.7	81.3	−67.5
$\{^1J_{C\text{-}1',H\text{-}1'}\}$	166.4	166.4	167.0	166.6
$\{^1J_{C\text{-}4,H\text{-}4}\}$	144.5	144.5	144.1	148.3
$\{^3J_{C\text{-}4,H\text{-}1'}\}$	3.9	3.3	5.2	5.2
$\{^3J_{C\text{-}1',H\text{-}4}\}$	4.9	5.1	3.4	6.8

Table 4. Calculated Mole Fractions y/% of Stable Conformers and Average Values of the Carbon—Proton Coupling Constants $^3J_{C,H}$/Hz for Lewis a (*II*) in Vacuum and Solution

	Vacuum	1,4-Dioxane	Methanol	DMSO	Water
y(LA1)	46.6	39.9	25.7	32.6	13.6
y(LA2)	37.9	45.1	59.6	52.9	68.1
y(LA3)	13.9	13.1	11.4	11.6	12.6
y(LA4)	1.6	1.9	3.3	2.9	5.7
$\langle\{^3J_{C\text{-}3,H\text{-}1'}\}\rangle$	3.8	3.8	3.8	3.8	3.7
$\langle\{^3J_{C\text{-}1',H\text{-}3}\}\rangle$	5.7	5.6	5.4	5.5	5.2
$\langle\{^3J_{C\text{-}4,H\text{-}1'}\}\rangle$	3.9	3.8	3.7	3.8	3.7
$\langle\{^3J_{C\text{-}1',H\text{-}4}\}\rangle$	4.8	4.8	4.9	4.8	4.9

Comparison of the calculated structure with the solid state experimental data is in this case difficult. The only crystal structure which can be compared with Lewis a is that in the complex of the tetrasaccharide α-L-Fuc-(1→2)-β-D-Gal-(1→3)-[α-L-Fuc-(1→4)]-β-D-GlcNAc and plant lectin, *Griffonia simplicifolia* isolectin IV [40]. The Lewis a trisaccharide moiety of tetrasaccharide in this complex adopts a conformation which resembles that in the minimum LA1 and is characterized by dihedral angles $\Phi = -64°$ and $\Psi = 138°$ for β-D-Gal-(1→3)-β-D-GlcNAc linkage and $\Phi = -63°$ and $\Psi = -88°$ for α-L-Fuc-(1→4)-β-D-GlcNAc linkage.

The populations of four minima in vacuum and solution are given in Table 4. It can be seen that the solvent effect shifted conformational equilibrium and the LA2 appeared to be the favoured minimum in solution. The abundance of the LA1 drops from 47 % in vacuum to 14 % in water, whereas the abundance of the LA2 increases from 38 % to 68 %. For the LA3 and LA4 minima, only slight differences are observed though the abundance of LA4 is clearly larger in water than in vacuum. Generally, the largest changes of conformers abundances are observed in aqueous solution in comparison to vacuum. The obtained results suggest that the equilibrium mixture of several conformations exists in solution. This conformational heterogeneity appears inconsistent with the previous findings that have suggested a single conformer for Lewis a.

Conformational behaviour of Lewis a trisaccharide was studied experimentally by NMR spectroscopy. Various techniques have been applied and they have encountered difficulty in an interpretation of the data. Glycosidic torsion angles were deduced from observed NOE's [8, 17]. Recently, vicinal carbon—proton coupling constants $^3J_{C,H}$ were measured for Lewis a [17]. The values $^3J_{C\text{-}3,H\text{-}1'} = 3.8$—4.4 Hz and $^3J_{C\text{-}1',H\text{-}3} = 5.0$ Hz for β-D-Gal-(1→3)-β-D-GlcNAc linkage, and $^3J_{C\text{-}4,H\text{-}1'} = 4.0$ Hz and $^3J_{C\text{-}1',H\text{-}4} = 5.3$ Hz for α-L-Fuc-(1→4)-β-D-GlcNAc linkage, were determined from NMR spectra. The calculated average values of

Table 5. Initial and Optimized Glycosidic Torsion Angles $\Phi^H/°$, $\Psi^H/°$and Relative Energies $\Delta E/(\text{kJ mol}^{-1})$ for Disaccharide Components of Lewis x (*III*) Conformers

		Initial				Optimized				
		β-D-Gal-(1→4)-β-D-GlcNAc		α-L-Fuc-(1→3)-β-D-GlcNAc		β-D-Gal-(1→4)-β-D-GlcNAc		α-L-Fuc-(1→3)-β-D-GlcNAc		
		$\{\Phi^H\}$	$\{\Psi^H\}$	$\{\Phi^H\}$	$\{\Psi^H\}$	$\{\Phi^H\}$	$\{\Psi^H\}$	$\{\Phi^H\}$	$\{\Psi^H\}$	$\{\Delta E\}$
1	B1, F1	36.6	−59.3	13.7	−27.4	35.3	169.3	16.2	−24.5	18.3
2	B1, F2	36.6	−59.3	16.4	30.0	converged to 8				
3	B1, F3	36.6	−59.3	69.1	68.5	44.9	−175.0	17.6	171.2	31.0
4	B1, F4	36.6	−59.3	10.7	175.5	converged to 8				
5	B2, F1	43.9	−6.5	13.7	−27.4	converged to 7				
6	B2, F2	43.9	−6.5	16.4	30.0	converged to 7				
7	B2, F3	43.9	−6.5	69.1	68.5	50.0	14.9	32.1	22.9	0.0
8	B2, F4	43.9	−6.5	10.7	175.5	56.8	20.3	22.7	−175.3	21.6
9	B3, F1	179.1	−2.6	13.7	−27.4	152.7	18.2	−24.2	−23.2	31.1
10	B3, F2	179.1	−2.6	16.4	30.0	177.6	7.1	33.9	28.7	41.4
11	B3, F3	179.1	−2.6	69.1	68.5	176.5	4.2	68.2	76.6	48.3
12	B3, F4	179.1	−2.6	10.7	175.5	converged to 8				
13	B4, F1	5.6	−174.2	13.7	−27.4	67.7	−161.0	20.4	31.6	29.7
14	B4, F2	5.6	−174.2	16.4	30.0	converged to 1				
15	B4, F3	5.6	−174.2	69.1	68.5	24.9	−175.1	60.2	79.8	49.7
16	B4, F4	5.6	−174.2	10.7	175.5	converged to 3				

$\langle {}^3J_{C,H}\rangle$ based on the population of minima and appropriate Karplus-type curve [28] are given in Table 4. Comparison of these values, $\langle {}^3J_{C\text{-}3,H\text{-}1'}\rangle$ = 3.7 Hz and $\langle {}^3J_{C\text{-}1',H\text{-}3}\rangle$ = 5.2 Hz for β-D-Gal-(1→3)-β-D-GlcNAc linkage, and $\langle {}^3J_{C\text{-}4,H\text{-}1'}\rangle$ = 3.7 Hz and $\langle {}^3J_{C\text{-}1',H\text{-}4}\rangle$ = 4.9 Hz for α-L-Fuc-(1→4)-β-D-GlcNAc linkage, with experimentally measured values showed that calculated average values are in a very good agreement with experimentally derived parameters. Since the average structure does not correspond to any of the individual minimum, Lewis a can be described as a flexible molecule.

Solution Structure of the Lewis x Trisaccharide (*III*)

Similarly as for the Lewis a trisaccharide, the starting conformations of the trisaccharide Lewis x (β-D-Gal-(1→4)-[α-L-Fuc-(1→3)]-β-D-GlcNAc) were constructed from the four minima found for both the β-D-Gal-(1→4)-β-D-GlcNAc (B1—B4) and α-L-Fuc-(1→4)-β-D-GlcNAc (F1—F4) disaccharides [24]. Combination of these minima gave 16 starting structures. Each trisaccharide structure was then subjected to further refinement of side groups orientation and geometry optimization. The results are shown in Table 5. It can be seen that from 16 starting conformers, 9 different minima for *III* were obtained. Consequently, four of the 9 optimized minima gave minimized energies that were within 30 kJ mol^{-1}. Summary of these energies and geometrical characteristics of the four lowest-energy minima is given in Table 6. It is noteworthy that the energies of two lowest-energy minima differ by 18 kJ mol^{-1}. This is a rather great difference in comparison to that found for the Lewis a trisaccharide. Comparison of Lewis x torsion angles with those of disaccharides showed that Φ and Ψ torsion angles of glycosidic linkages in Lewis x deviated more from the disaccharide values than in Lewis a. Furthermore, in the lowest-energy conformer for Lewis x, the conformation of both disaccharide segments is significantly shifted from the lowest-energy conformer of the given linkage. This suggests that the presence of the α-L-Fuc in the position C-3 of the β-D-GlcNAc limits flexibility of the Lewis x more than the presence of α-L-Fuc at C-4 in the Lewis a. Similar findings followed from recent molecular modelling study of histo-blood group oligosaccharides, where one family of conformers has been predicted for the Lewis x but two families of conformers were observed for the Lewis a [21].

Calculated mole fractions of conformers in vacuum and solution together with average values of carbon—proton couplings $\langle {}^nJ_{C,H}\rangle$ are compared in Table 7. The vacuum lowest-energy conformer LX1 is favoured in all solvents. However, the population of this minimum decreases from 100 % in vacuum to 78 % in aqueous solution. On the contrary, the abundance of the LX2 and LX4 conformers increases to 13 % and 8 %, respectively. A larger flexibility of Lewis x predicted for aqueous solution has only a small influence on average values of $\langle {}^nJ_{C,H}\rangle$. Vacuum equilibrium is characterized by the average values $\langle {}^3J_{C\text{-}4,H\text{-}1'}\rangle$ = 2.5 Hz and $\langle {}^3J_{C\text{-}1',H\text{-}4}\rangle$ = 5.2 Hz for the β-D-Gal-(1→4)-β-D-GlcNAc linkage and $\langle {}^3J_{C\text{-}3,H\text{-}1'}\rangle$ = 4.1 Hz, $\langle {}^3J_{C\text{-}1',H\text{-}3}\rangle$= 4.8 Hz for α-L-Fuc-(1→3)-β-D-GlcNAc linkage. For aqueous solution similar values, $\langle {}^3J_{C\text{-}4,H\text{-}1'}\rangle$= 2.5 Hz and $\langle {}^3J_{C\text{-}1',H\text{-}4}\rangle$ = 5.5 Hz for the β-D-Gal-(1→4)-β-D-GlcNAc linkage and $\langle {}^3J_{C\text{-}3,H\text{-}1'}\rangle$ = 4.3 Hz, $\langle {}^3J_{C\text{-}1',H\text{-}3}\rangle$

Table 6. Numerical Values of Relative Energies ΔE/(kJ mol^{-1}), Dipole Moments μ/D, Torsion Angles $\Phi^H/°$, $\Psi^H/°$, $\Phi/°$, $\Psi/°$, and Carbon—Proton Coupling Constants $^1J_{C,H}$/Hz and $^3J_{C,H}$/Hz Calculated for the Minima of Lewis x (*III*)

	LX1	LX2	LX3	LX4
$\{\Delta E\}$	0.00	18.31	21.63	29.67
$\{\mu\}$	5.5	9.4	5.1	11.6
		β-D-Gal-(1→4)-β-D-GlcNAc		
$\{\Phi^H\}$	50.0	35.3	56.8	67.7
$\{\Psi^H\}$	14.9	169.3	20.3	−161.0
$\{\Phi\}$	−69.9	−84.7	−62.7	−52.8
$\{\Psi\}$	134.8	−76.0	142.0	−45.3
$\{^1J_{C\text{-}1',H\text{-}1'}\}$	159.6	159.6	159.6	159.6
$\{^1J_{C\text{-}4,H\text{-}4}\}$	144.1	145.8	144.1	146.8
$\{^3J_{C\text{-}4,H\text{-}1'}\}$	2.5	3.8	1.9	1.1
$\{^3J_{C\text{-}1',H\text{-}4}\}$	5.2	6.6	5.0	6.2
		α-L-Fuc-(1→3)-β-D-GlcNAc		
$\{\Phi^H\}$	32.1	16.2	22.7	20.4
$\{\Psi^H\}$	22.9	−24.5	−175.3	31.6
$\{\Phi\}$	−85.5	−101.6	−93.3	−96.6
$\{\Psi\}$	−98.8	−139.3	69.9	−89.8
$\{^1J_{C\text{-}1',H\text{-}1'}\}$	166.4	166.6	166.5	166.5
$\{^1J_{C\text{-}3,H\text{-}3}\}$	144.5	144.4	148.2	144.4
$\{^3J_{C\text{-}3,H\text{-}1'}\}$	4.1	5.2	4.8	4.9
$\{^3J_{C\text{-}1',H\text{-}3}\}$	4.8	4.7	6.8	4.1

Table 7. Calculated Mole Fractions y/% of Stable Conformers and Average Values of the Carbon—Proton Coupling Constants $^3J_{C,H}$/Hz for Lewis x (*III*) in Vacuum and Solution

	Vacuum	1,4-Dioxane	Methanol	DMSO	Water
y(LX1)	99.9	99.8	96.7	98.5	77.5
y(LX2)	0.1	0.2	2.7	1.3	13.7
y(LX3)	0.0	0.0	0.1	0.1	0.2
y(LX4)	0.0	0.0	0.5	0.1	8.6
$\langle\{^3J_{C\text{-}4,H\text{-}1'}\}\rangle$	2.5	2.5	2.5	2.5	2.5
$\langle\{^3J_{C\text{-}1',H\text{-}4}\}\rangle$	5.2	5.2	5.3	5.3	5.5
$\langle\{^3J_{C\text{-}3,H\text{-}1'}\}\rangle$	4.1	4.1	4.1	4.1	4.3
$\langle\{^3J_{C\text{-}1',H\text{-}3}\}\rangle$	4.8	4.8	4.8	4.8	4.7

= 4.7 Hz for α-L-Fuc-(1→3)-β-D-GlcNAc linkage, were obtained. The calculated value of $\langle^3J_{C\text{-}1',H\text{-}4}\rangle$ = 5.5 Hz for the β-D-Gal-(1→4)-β-D-GlcNAc linkage is in a very good agreement with the only experimentally available coupling constant $^3J_{C\text{-}1',H\text{-}4}$ = 5.4 Hz [12]. Experimental studies [12—14] implied a single conformation with a very limited flexibility. In these studies NMR data are often used as constraints applied to energy minimization or to molecular dynamic simulation and therefore the existence of one conformation is inherent to the procedure. Nevertheless, the structure inferred from NMR data is similar to the LX1 conformer.

Solution Structure of the Sialyl Lewis a Tetrasaccharide (*IV*)

Totally 50 starting structures of the tetrasaccharide sialyl Lewis a α-D-Neu5Ac-(2→3)-β-D-Gal-(1→3)-[α-L-Fuc-(1→4)]-β-D-GlcNAc were built by a combination of 10 minima of the Lewis a trisaccharide (LA1—LA10) and 5 minima of the α-D-Neu5Ac-(2→3)-β-D-Gal disaccharide (S1—S5). Their geometry optimization was performed as for trisaccharides *II* and *III*. This led to 24 conformers for sialyl Lewis a with 15 of them within the relative energy of 30 kJ mol^{-1} (Table 8). Five of these minima appeared to be populated more than 1 % at least in one of the assumed solvents. The relative energy and geometrical characteristics of these minima described as SLA1—SLA5 are given in Table 9. The energy difference between two lowest-energy conformers SLA1 and SLA2 is 1.95 kJ mol^{-1}. However, a larger energy gap is observed for other minima. The relative energies of the minima SLA3, SLA4, and SLA5 are 15.91 kJ mol^{-1}, 24.21 kJ mol^{-1}, and 42.82 kJ mol^{-1}, respectively. Comparison of the lowest-energy conformer for sialyl Lewis a with its precursor Lewis a indicates that the addition of sialic acid to Lewis a trisaccharide influences the orientation around glycosidic linkages. In all conformers of *IV*, the orientation around glycosidic linkages differs from those found in Lewis a. However,

Table 8. Optimized Glycosidic Torsion Angles Φ^H/°, Ψ^H/°and Relative Energies ΔE/(kJ mol^{-1}) of Sialyl Lewis a (*IV*) Conformers

		β-D-Gal-(1→3)-β-D-GlcNAc		α-L-Fuc-(1→4)-β-D-GlcNAc		α-D-Neu5Ac-(2→3)-β-D-Gal		
		$\{\Phi^H\}$	$\{\Psi^H\}$	$\{\Phi^H\}$	$\{\Psi^H\}$	$\{\Phi^C\}$	$\{\Psi^H\}$	$\{\Delta E\}$
1	LA6, S1	91	54	11	−43	−45	57	0.0
2	LA4, S1	41	−179	18	174	−32	53	1.9
3	LA2, S2	39	12	76	46	−58	3	15.9
4	LA2, S1	35	23	43	18	−43	69	18.4
5	LA5, S1	32	26	19	152	−39	57	21.2
6	LA1, S2	40	−177	32	−24	−103	29	21.5
7	LA2, S5	41	17	42	19	63	11	22.3
8	LA5, S2	38	30	16	156	−100	25	22.4
9	LA2, S4	34	22	42	19	−163	−19	24.2
10	LA2, S3	33	18	60	34	−63	141	24.3
11	LA1, S5	24	175	35	−18	75	47	25.8
12	LA6, S5	87	54	19	−49	65	68	27.4
13	LA4, S5	35	180	14	177	46	31	29.2
14	LA3, S1	31	16	−25	−34	−46	52	29.9
15	LA1, S4	35	175	35	−19	−171	−13	30.0
16	LA1, S1	35	173	36	−14	−34	34	31.2
17	LA4, S4	45	−176	23	172	−171	−14	33.7
18	LA4, S2	43	−176	26	168	−87	29	33.9
19	LA1, S3	25	175	36	−18	−66	141	38.3
20	LA6, S2	79	58	25	−50	−91	22	39.9
21	LA5, S4	27	30	16	160	−163	−19	42.8
22	LA3, S3	36	25	−17	−39	−70	141	47.1
23	LA4, S3	44	−173	22	171	−63	143	48.5
24	LA6, S4	82	58	26	−49	−164	−19	49.1

Table 9. Numerical Values of Relative Energies ΔE/(kJ mol^{-1}), Dipole Moments μ/*D*, Torsion Angles Φ^H/°, Ψ^H/°, Φ/°, Ψ/°, and Carbon—Proton Coupling Constants $^1J_{C,H}$/Hz and $^3J_{C,H}$/Hz Calculated for the Minima of Sialyl Lewis a (*IV*)

	SLA1	SLA2	SLA3	SLA4	SLA5
$\{\Delta E\}$	0.00	1.95	15.91	24.21	42.82
$\{\mu\}$	4.0	7.4	13.7	12.2	13.2
		β-D-Gal-(1→3)-β-D-GlcNAc			
$\{\Phi^H\}$	91.1	41.1	38.7	33.8	27.1
$\{\Psi^H\}$	53.9	−178.8	12.3	22.4	30.3
$\{\Phi\}$	−27.1	−78.3	−80.2	−84.9	−90.6
$\{\Psi\}$	−69.6	67.2	−107.6	−98.9	−91.8
$\{^1J_{C\text{-}1',H\text{-}1'}\}$	159.4	159.6	159.6	159.5	159.4
$\{^1J_{C\text{-}3,H\text{-}3}\}$	144.2	146.3	144.1	144.1	144.1
$\{^3J_{C\text{-}3,H\text{-}1'}\}$	0.5	3.3	3.5	3.9	4.5
$\{^3J_{C\text{-}1',H\text{-}3}\}$	2.1	6.8	5.4	4.8	4.2
		α-L-Fuc-(1→4)-β-D-GlcNAc			
$\{\Phi^H\}$	11.0	17.9	76.1	41.9	16.2
$\{\Psi^H\}$	−42.7	173.8	45.7	19.5	159.8
$\{\Phi\}$	−106.4	−99.6	−43.3	−75.5	−103.5
$\{\Psi\}$	79.7	−70.7	162.0	139.0	−87.7
$\{^1J_{C\text{-}1',H\text{-}1'}\}$	166.7	166.6	167.7	166.4	166.6
$\{^1J_{C\text{-}4,H\text{-}4}\}$	144.1	148.3	144.2	144.5	148.2
$\{^3J_{C\text{-}4,H\text{-}1'}\}$	5.4	5.1	0.7	3.2	5.2
$\{^3J_{C\text{-}1',H\text{-}4}\}$	3.1	6.7	2.9	5.0	6.1
		α-D-Neu5Ac-(2→3)-β-D-Gal			
$\{\Phi^C\}$	−45.3	−32.2	−57.7	−162.7	−162.9
$\{\Psi^H\}$	56.9	53.2	3.1	−19.4	−19.4
$\{\Phi\}$	78.0	90.6	63.2	−46.8	−47.0
$\{\Psi\}$	−67.0	−72.6	−118.0	−139.0	−139.2
$\{^1J_{C\text{-}3,H\text{-}3}\}$	144.2	144.2	144.6	144.5	144.5
$\{^3J_{C\text{-}2',H\text{-}3}\}$	1.9	2.2	5.6	5.0	5.0

Table 10. Calculated Mole Fractions y/% of Stable Conformers and Average Values of the Carbon—Proton Coupling Constants $^3J_{C,H}$/Hz for Sialyl Lewis a (*IV*) in Vacuum and Solution

	Vacuum	1,4-Dioxane	Methanol	DMSO	Water
y(SLA1)	68.5	56.8	8.1	22.7	0.3
y(SLA2)	31.4	41.6	14.2	34.3	0.6
y(SLA3)	0.1	1.5	76.6	42.6	94.1
y(SLA4)	0.0	0.1	1.0	0.4	0.5
y(SLA5)	0.0	0.0	0.1	0.0	4.5
$\langle\{^3J_{C\text{-}3,H\text{-}1'}\}\rangle$	1.4	1.7	3.2	2.8	3.5
$\langle\{^3J_{C\text{-}1',H\text{-}3}\}\rangle$	3.6	4.1	5.3	5.1	5.3
$\langle\{^3J_{C\text{-}4,H\text{-}1'}\}\rangle$	5.3	5.2	1.7	3.3	0.9
$\langle\{^3J_{C\text{-}1',H\text{-}4}\}\rangle$	4.3	4.6	3.5	4.3	3.0
$\langle\{^3J_{C\text{-}2',H\text{-}3}\}\rangle$	2.0	2.1	4.8	3.6	5.5

Table 11. Optimized Glycosidic Torsion Angles Φ^H/°, Ψ^H/°and Relative Energies ΔE/(kJ mol^{-1}) of Sialyl Lewis x (*V*) Conformers

		β-D-Gal-(1→4)-β-D-GlcNAc		α-L-Fuc-(1→3)-β-D-GlcNAc		α-D-Neu5Ac-(2→3)-β-D-Gal		
		$\{\Phi^H\}$	$\{\Psi^H\}$	$\{\Phi^H\}$	$\{\Psi^H\}$	$\{\Phi^C\}$	$\{\Psi^H\}$	$\{\Delta E\}$
1	LX5, S2	24	−177	22	171	−62	10	0.0
2	LX5, S1	33	174	17	173	−44	56	0.9
3	LX5, S3	13	174	18	177	−64	138	10.2
4	LX2, S2	34	168	14	−23	−56	−3	13.6
5	LX1, S3	45	16	33	24	−57	138	14.1
6	LX1, S1	50	15	32	22	−35	51	14.8
7	LX1, S4	47	14	32	24	−165	−15	17.6
8	LX1, S2	48	13	32	23	−59	13	18.8
9	LX3, S1	61	25	24	178	−40	63	20.3
10	LX1, S5	49	16	31	23	58	17	20.6
11	LX3, S3	62	25	23	177	−60	120	27.2
12	LX3, S4	58	26	25	179	−168	−16	29.6
13	LX2, S1	29	164	23	−16	−36	52	30.3
14	LX2, S3	37	165	16	−19	−65	137	30.8
15	LX3, S5	55	28	25	179	57	16	31.0
16	LX3, S2	50	28	25	180	−60	10	31.6
17	LX4, S2	58	−164	23	39	−58	8	34.2
18	LX5, S5	19	176	21	173	58	24	36.4
19	LX4, S1	66	−165	22	33	−35	56	36.8
20	LX2, S4	36	164	17	−19	−171	−11	38.3
21	LX4, S4	65	−163	21	36	−171	−8	44.4
22	LX5, S4	22	170	15	174	−170	−12	45.0
23	LX2, S5	23	163	24	−8	53	26	46.1
24	LX4, S3	78	−169	24	29	−63	132	46.8
25	LX4, S5	68	−165	23	32	58	17	48.8

conformation about linkage between the α-D-Neu5Ac and β-D-Gal corresponds to the two lowest-energy conformers of the α-D-Neu5Ac-(2→3)-β-D-Gal disaccharide.

The abundance of five conformers in vacuum and in solution is given in Table 10. In vacuum, only two lowest-energy conformers were presented in the equilibrium. The mole fractions of conformers alter significantly in solution. It appeared that with an increase of solvent polarity, the equilibrium is shifted towards the SLA3. The abundance of the SLA3 increases from 0.1 % in vacuum through 42.6 % in dimethyl sulfoxide and 76.6 % in methanol to 94.1 % in water. In aqueous solution, the second lowest-energy conformer is the SLX5 with the abundance of 4.5 %. Comparison of conformations for trisaccharide Lewis a and tetrasaccharide sialyl Lewis a revealed interesting differences. The pattern of glycosidic torsion angles characteristic of the lowest-energy conformer of the Lewis a has not been found in the lowest-energy conformers of the sialyl Lewis a. In water, the highest populated conformation for Lewis a is LA2. Corresponding conformation in the tetrasaccharide is SLA4, but this conformer has only negligible popula-

Table 12. Numerical Values of Relative Energies ΔE/(kJ mol^{-1}), Dipole Moments μ/D, Torsion Angles Φ^H/°, Ψ^H/°, Φ/°, Ψ/°, and Carbon—Proton Coupling Constants $^1J_{C,H}$/Hz and $^3J_{C,H}$/Hz Calculated for the Minima of Sialyl Lewis x (V)

	SLX1	SLX2	SLX3	SLX4	SLX5
$\{\Delta E\}$	0.00	0.94	10.23	17.64	18.84
$\{\mu\}$	10.0	9.2	14.2	11.3	15.4
		β-D-Gal-(1→4)-β-D-GlcNAc			
$\{\Phi^H\}$	23.7	33.4	13.3	46.8	47.7
$\{\Psi^H\}$	−177.3	174.4	174.2	13.7	13.4
$\{\Phi\}$	−94.8	−85.8	−104.9	−72.4	−71.7
$\{\Psi\}$	−61.5	−68.2	−68.5	133.6	133.3
$\{^1J_{C\text{-}1',H\text{-}1'}\}$	159.3	159.5	159.1	159.6	159.6
$\{^1J_{C\text{-}4,H\text{-}4}\}$	146.3	146.0	146.0	144.1	144.1
$\{^3J_{C\text{-}4,H\text{-}1'}\}$	4.7	4.0	5.3	2.8	2.7
$\{^3J_{C\text{-}1',H\text{-}4}\}$	6.8	6.7	6.7	5.3	5.3
		α-L-Fuc-(1→3)-β-D-GlcNAc			
$\{\Phi^H\}$	22.0	16.8	18.5	32.1	32.4
$\{\Psi^H\}$	171.0	172.6	177.2	24.2	23.0
$\{\Phi\}$	−95.6	−100.5	−98.9	−85.5	−85.4
$\{\Psi\}$	58.6	58.9	62.7	−97.6	−98.8
$\{^1J_{C\text{-}1',H\text{-}1'}\}$	166.5	166.6	166.6	166.4	166.4
$\{^1J_{C\text{-}3,H\text{-}3}\}$	148.3	148.3	148.3	144.5	144.5
$\{^3J_{C\text{-}3,H\text{-}1'}\}$	4.8	5.1	5.1	4.1	4.1
$\{^3J_{C\text{-}1',H\text{-}3}\}$	6.7	6.7	6.8	4.7	4.8
		α-D-Neu5Ac-(2→3)-β-D-Gal			
$\{\Phi^C\}$	−62.4	−44.0	−63.7	−164.6	−58.8
$\{\Psi^H\}$	10.4	56.1	138.5	−15.5	12.7
$\{\Phi\}$	57.5	78.7	59.8	−48.6	62.0
$\{\Psi\}$	−112.5	−67.9	19.6	−135.6	−110.0
$\{^1J_{C\text{-}3,H\text{-}3}\}$	144.6	144.2	147.4	144.5	144.6
$\{^3J_{C\text{-}2',H\text{-}3}\}$	5.4	1.9	4.1	5.2	5.3

tion. The most populated conformer SLA3 is also similar to the LA2. The LA2 and SLA3 conformers differ mainly at α-L-Fuc-(1→4)-β-D-GlcNAc linkage where the Φ^H, Ψ^H torsion angles are shifted about 30°. Thus, in water both lowest-energy conformations SLA3 and SLA4 are derived from the same trisaccharide conformer LA2 and they differ mainly in orientation of the sialic acid residue. This suggests that sialylation of the trisaccharide Lewis a restricts the flexibility of glycosidic linkages in this moiety and that the change of the orientation about the α-D-Neu5Ac-(2→3)-β-D-Gal linkage causes conformational changes about the α-L-Fuc-(1→4)-β-D-GlcNAc linkage. As expected from the large solvent dependence of the population of conformers, significant differences in average values $\langle^3J_{C,H}\rangle$ can be observed in the given solvents (Table 10). The following average coupling constants were calculated for aqueous solution: $\langle^3J_{C\text{-}3,H\text{-}1'}\rangle$ = 3.5 Hz and $\langle^3J_{C\text{-}1',H\text{-}3}\rangle$ = 5.3 Hz for the β-D-Gal-(1→3)-β-D-GlcNAc linkage, $\langle^3J_{C\text{-}4,H\text{-}1'}\rangle$ = 0.9 Hz and $\langle^3J_{C\text{-}1',H\text{-}4}\rangle$= 3.0 Hz for the α-L-Fuc-(1→4)-β-D-GlcNAc linkage and $\langle^3J_{C\text{-}2',H\text{-}3}\rangle$ = 5.5 Hz for the α-D-Neu5Ac-(2→3)-β-D-Gal linkage.

Solution Structure of the Sialyl Lewis x Tetrasaccharide (V)

For the sialyl Lewis x tetrasaccharide (α-D-Neu5Ac-(2→3)-β-D-Gal-(1→4)-[α-L-Fuc-(1→3)]-β-D-GlcNAc), the starting conformations were generated using results from the trisaccharide Lewis x and the disaccharide α-D-Neu5Ac-(2→3)-β-D-Gal. Thus, five minima (S1—S5) were used for the α-D-Neu5Ac-(2→3)-β-D-Gal linkage and nine minima were used for the Lewis x trisaccharide (LX1—LX9), to give a total of 45 combinations of sialyl Lewis x starting conformations. The optimization of these structures led to 25 different minima (Table 11), with 12 conformers within the relative energy of 30 kJ mol^{-1}. Descriptions of the five lowest-energy minima that occur in equilibrium mixture and their energetics are found in Table 12. These minima have relative energies within 19 kJ mol^{-1}. Two groups of conformers can be recognized between the minima of the sialyl Lewis x tetrasaccharide. The first group includes minima LX1, LX2, and LX3 and is characterized by the *trans* orientation of Ψ^H torsion angle on β-D-Gal-(1→4)-β-D-GlcNAc and α-L-Fuc-(1→3)-β-D-GlcNAc linkages. The second group contains two conformers, SLX4 and SLX5. These minima differ only in the orientation of sialic acid, but orientation about remaining two glycosidic linkages is the same.

Abundances of conformers presented in Table 13 suggest that an equilibrium between several conformations exists in solution. This equilibrium appears to be very sensitive to solvent. It can be seen that two conformers, SLX1 (58 %) and SLX2 (40 %), are dominant in vacuum, whereas in water, the equilibrium

Table 13. Calculated Mole Fractions y/% of Stable Conformers and Average Values of the Carbon—Proton Coupling Constants $^3J_{C,H}$/Hz for Sialyl Lewis x (V) in Vacuum and Solution

	Vacuum	1,4-Dioxane	Methanol	DMSO	Water
y(SLX1)	58.7	66.7	31.5	52.4	2.0
y(SLX2)	40.2	28.1	4.0	10.3	0.1
y(SLX3)	1.0	4.1	26.4	22.9	3.9
y(SLX4)	0.1	0.7	1.6	1.5	5.7
y(SLX5)	0.0	0.4	36.5	12.9	88.3
$\langle\{^3J_{C\text{-}4,H\text{-}1'}\}\rangle$	4.4	4.5	4.1	4.5	2.8
$\langle\{^3J_{C\text{-}1',H\text{-}4}\}\rangle$	6.8	6.8	6.2	6.6	5.4
$\langle\{^3J_{C\text{-}3,H\text{-}1'}\}\rangle$	5.0	4.9	4.6	4.8	4.1
$\langle\{^3J_{C\text{-}1',H\text{-}3}\}\rangle$	6.7	6.7	6.0	6.4	4.9
$\langle\{^3J_{C\text{-}2',H\text{-}3}\}\rangle$	4.0	4.4	4.9	4.8	5.3

is significantly shifted towards the SLX5 (88 %). For methanol and dimethyl sulfoxide solution, all minima are more evenly distributed. Not surprisingly, calculated average values based on the population of minima are solvent-dependent. Recently measured [11, 12, 18] vicinal carbon—proton coupling constants $^3J_{C,H}$ provide a reasonable set of experimental data that can be used to estimate how reliable is the predicted equilibrium. The values $^3J_{C\text{-}4,H\text{-}1'}$ = 2.8 Hz, $^3J_{C\text{-}1',H\text{-}4}$ = 4.8 Hz for the β-D-Gal-(1→4)-β-D-GlcNAc linkage, $^3J_{C\text{-}3,H\text{-}1'}$ = 2.8 Hz, $^3J_{C\text{-}1',H\text{-}3}$ = 5.0—5.2 Hz for the α-L-Fuc-(1→3)-β-D-GlcNAc linkage, and $^3J_{C\text{-}2',H\text{-}3}$ = 5.4 Hz for the α-D-Neu5Ac-(2→3)-β-D-Gal linkage were determined from the NMR spectra. From the mole fractions and individual vicinal coupling constants, the following average coupling constants in aqueous solution have been calculated: $\langle^3J_{C\text{-}4,H\text{-}1'}\rangle$ = 2.8 Hz, $\langle^3J_{C\text{-}1',H\text{-}4}\rangle$ = 5.4 Hz for the β-D-Gal-(1→4)-β-D-GlcNAc linkage, $\langle^3J_{C\text{-}3,H\text{-}1'}\rangle$ = 4.1 Hz, $\langle^3J_{C\text{-}1',H\text{-}3}\rangle$ = 4.9 Hz for the α-L-Fuc-(1→3)-β-D-GlcNAc linkage, and $\langle^3J_{C\text{-}2',H\text{-}3}\rangle$ = 5.3 Hz for the α-D-Neu5Ac-(2→3)-β-D-Gal linkage. Four of the five calculated average values of $^3J_{C,H}$ agreed with the measured values within the limit of the experimental error (± 0.5 Hz). Difference between the calculated and experimental value of $^3J_{C\text{-}3,H\text{-}1'}$ coupling constant (4.1 Hz *vs.* 2.8 Hz) represents approximately 10° in the Φ^H torsion angle for α-L-Fuc-(1→3)-β-D-GlcNAc linkage. Therefore, the predicted equilibrium of conformers for sialyl Lewis x is in a satisfactory agreement with experiment.

CONCLUSION

As the blood determinants are involved in a number of cell surface recognition processes, we have modelled the conformational behaviour of the trisaccharides Lewis a, Lewis x, and their sialylated derivatives sialyl Lewis a and sialyl Lewis x in solution. The RAMM procedure associated with the solvation energy estimation used in this work allowed us to explore the influence of the side group orientation on the available conformational space and to investigate solvent effects on the conformational equilibrium of minima. Calculated average values of vicinal carbon—proton coupling constants ($^3J_{C,H}$) were found to be in a good agreement with available experimental data and support the reliability of predicted conformational properties of these compounds. The predicted conformational flexibilities of studied molecules are larger than assumed up to now. An apparent conformational flexibility suggests that interactions between the oligosaccharides of the blood-group antigens and proteins or small molecules may involve conformational transitions that stabilize the resulting complex.

Acknowledgements. This investigation was supported by the grant No. 2/1235/94 from the Slovak Grant Agency for Science.

REFERENCES

1. Varki, A., *Glycobiology 3,* 97 (1993).
2. Phillips, M. L., Nudelman, E., Gaeta, C. A., Perez, M., Singhai, A. K., Hakomori, S. I., and Paulson, J. C., *Science 250,* 1130 (1990).
3. Berg, E. L., Robinson, M. K., Mansson, O., Butcher, E. C., and Magnani, J. L., *J. Biol. Chem. 266,* 14869 (1991).
4. Lasky, L. A., *Science 258,* 964 (1992).
5. Lemieux, R. U., Bock, K., Delbaere, L. T. J., Koto, S., and Rao, V. S., *Can. J. Chem. 58,* 631 (1980).
6. Biswas, M. and Rao, V. S. R., *Carbohydr. Polymer 2,* 205 (1982).
7. Hounsel, E. F., Jones, N. J., Goot, H. C., and Feizi, T., *Carbohydr. Res. 178,* 67 (1988).
8. Cagas, P. and Bush, C. A., *Biopolymers 30,* 1123 (1990).
9. Mukhopadhyay, C. and Bush, C. A., *Biopolymers 31,* 1737 (1991).
10. Ball, E. G., O'Neill, R. A., Schultz, J. E., Lowe, J. B., Weston, B. W., Nagy, J. O., Brown, E. G., Hobbs, C. J., and Bednarski, M. D., *J. Am. Chem. Soc. 114,* 5449 (1992).
11. Lin, Y.-C., Hummel, C. W., Huang, D.-H., Ichikawa, Y., Nicolaou, K. C., and Wong, C.-H., *J. Am. Chem. Soc. 114,* 5452 (1992).
12. Ichikawa, Y., Lin, Y.-C., Dumas, D. P., Shen, G.-J., Garcia-Junceda, E., Williams, M. A., Bayer, R.,

Ketcham, C., Walker, L. E., Paulson, J. C., and Wong, C.-H., *J. Am. Chem. Soc. 114,* 9283 (1992).
13. Miller, K. E., Mukhopadhyay, C., Cagas, P., and Bush, C. A., *Biochemistry 31,* 6703 (1992).
14. Homans, S. W. and Forster, M., *Glycobiology 2,* 143 (1992).
15. Wormald, M. R. and Edge, C. J., *Carbohydr. Res. 246,* 337 (1993).
16. Mukhopadhyay, C., Miller, K. E., and Bush, C. A., *Biopolymers 34,* 21 (1994).
17. Kogelberg, H. and Rutherford, T. J., *Glycobiology 4,* 49 (1994).
18. Rutherford, T. J., Spackman, D. G., Simpson, P. J., and Homans, S. W., *Glycobiology 4,* 59 (1994).
19. Coteron, J. M., Singh, K., Asensio, J. L., Dalda, M. D., Mayoralas, A. F., Barbero, J. J., and Lomas, M. M., *J. Org. Chem. 60,* 1502 (1995).
20. DeFrees, S. A., Kosch, W., Way, W., Paulson, J. C., Sabesan, S., Halcomb, R. L., Huang, D.-H., Ichikawa, Y., and Wong, C.-H., *J. Am. Chem. Soc. 117,* 66 (1995).
21. Imberty, A., Mikros, E., Koča, J., Mollicone, R., Oriol, R., and Perez, S., *Glycoconjugate J. 12,* 331 (1995).
22. Siebert, H. C., Reuter, G., Schauer, R., Lieth, C. W. v. d., and Dabrowski, J., *Biochemistry 31,* 6962 (1992).
23. Balaji, P. V., Qasba, P. K., and Rao, V. S. R., *Biochemistry 32,* 12599 (1993).
24. Bízik, F. and Tvaroška, I., *Chem. Papers 49,* 202 (1995).
25. Kožár, T., Petrák, F., Gálová, Z., and Tvaroška, I., *Carbohydr. Res. 204,* 27 (1990).
26. Burkert, U. and Allinger, N. L., *Molecular Mechanics.* American Chemical Society, Washington, D.C., 1982.
27. Tvaroška, I. and Kožár, T., *J. Am. Chem. Soc. 102,* 6929 (1980).
28. Tvaroška, I., Hricovíni, M., and Petráková, E., *Carbohydr. Res. 189,* 359 (1989).
29. Tvaroška, I. and Taravel, F. R., *Carbohydr. Res. 221,* 83 (1991).
30. Tvaroška, I. and Taravel, F. R., *J. Biomol. NMR 2,* 421 (1992).
31. Sabesan, S., Bock, K., and Paulson, J. C., *Carbohydr. Res. 218,* 27 (1991).
32. Mukhopadhyay, C., Miller, K. E., and Bush, C. A., *Biopolymers 34,* 11 (1994).
33. Poppe, L. and Dabrowski, J., *Biochem. Biophys. Res. Commun. 159,* 618 (1989).
34. Breg, J., Kroon-Batenburg, L. M. J., Strecker, G., Montreuil, J., and Vliegenthart, J. F. G., *Eur. J. Biochem. 178,* 727 (1989).
35. Bechtel, B., Wand, A. J., Wroblewski, K., Koprowski, H., and Thurin, J., *J. Biol. Chem. 265,* 2028 (1990).
36. Scarsdale, J. N., Prestegard, J. H., and Yu, R. K., *Biochemistry 29,* 9843 (1990).
37. Acquotti, D., Poppe, L., Dabrowski, J., Lieth, C.-W. v. d., Sonino, S., and Tettamanti, G., *J. Am. Chem. Soc. 112,* 7772 (1990).
38. Rodgers, J. C. and Portoghese, P. S., *Biopolymers 34,* 1311 (1994).
39. Tvaroška, I. and Bleha, T., *Adv. Carbohydr. Chem. Biochem. 47,* 45 (1989).
40. Delbaere, L. T. J., Vandonselaar, M., Prasad, L., Quail, J. W., Wilson, K. S., and Dauter, Z., *J. Mol. Biol. 230,* 950 (1993).

Translated by the authors